JOURNAL OF THERMOPHYSICS AND HEAT TRANSFER
Vol. 20, No. 2, April–June 2006

Thermal Interaction Between Two Vertical Systems of Free and Forced Convection

M. Mosaad* and M. Al-Hajeri†
P.O. Box 64268, Shuikh 70453, Kuwait

Conjugate heat transfer between two thermal systems of free and forced convection, separated by a vertical wall, is investigated theoretically. It is assumed that the heat conduction in the wall is only in the transversal direction. The situation considered is one in which the two vertical boundary layers of free and forced convection induced on wall sides are in counterflow. The study shows that the thermal interaction process between the two thermal systems is controlled by two dimensionless groups: The ζ parameter relates the heat transfer effectiveness of two convection layers, and ω parameter evaluates the wall thermal resistance to the forced-layer resistance. The obtained results explain the effects of these two parameters on the fluid–solid interfacial temperature at wall sides, the temperature fields in the solid and fluid regions, as well as the local and mean Nusselt numbers. Comparison is made between model predictions and numerical results obtained by FLUENT for special model problems.

Nomenclature

b	=	wall thickness
g	=	gravitational acceleration
h	=	heat transfer coefficient
k	=	thermal conductivity
L	=	wall height
l	=	scale of free convection-layer thickness
Nu_{xc}	=	local Nusselt number of cold, forced convection side, $h_{xc}x/k_c$
Nu_{xh}	=	local Nusselt number of hot, free convection side, $h_{xh}x/k_h$
$\overline{Nu}$	=	mean conjugate Nusselt number, $\bar{q}L/(k\Delta t)$
Pr	=	Prandtl number, ν/α
$\bar{q}$	=	mean heat flux over entire wall height
Ra	=	modified Rayleigh number, Eq. (12)
Ra_x	=	local Rayleigh number based on $(t_{h\infty} - t_{wh})$
Re_L	=	Reynolds number, $u_\infty L/\nu$
t	=	temperature
$t_{c\infty}$	=	free cold-fluid temperature
$t_{h\infty}$	=	free hot-fluid temperature
U, V	=	dimensionless velocity components in x- and y-directions, respectively
u, v	=	velocity components in x- and y-directions, respectively
X, Y	=	dimensionless vertical and horizontal coordinates
x, y	=	vertical and horizontal coordinates (Fig. 1)
α	=	thermal diffusivity
β	=	thermal expansion coefficient
Δ	=	dimensionless thickness of forced convection velocity layer
Δt	=	total temperature drop across two fluid media, $(t_{h\infty} - t_{c\infty})$
Δ_t	=	dimensionless thickness of forced convection thermal layer
δ	=	thickness of forced convection velocity layer
ζ	=	dimensionless conjugation parameter, Eq. (25)
η	=	inverse Oseen function $1/\lambda$
θ	=	dimensionless temperature
λ	=	Oseen function
ν	=	kinematic viscosity
ω	=	dimensionless wall parameter, Eq. (25)
$\oslash$	=	thickness ratio of thermal to velocity layer, Δ_t/Δ

Subscripts

c	=	cold fluid
h	=	hot fluid
w	=	wall
wc	=	wall–fluid interface of cold-fluid side
wh	=	wall–fluid interface of hot-fluid side
x	=	local value

Received 19 October 2004; revision received 23 February 2005; accepted for publication 3 June 2005.

*Associate Professor, Faculty of Technical Studies, Mechanical Power Department; on leave from Mansoura University of Egypt; mosaad77@hotmail.com.

†Associate Professor, Faculty of Technical Studies, Mechanical Power Department; alhajery@hotmail.com.

I. Introduction

CONVECTIVE heat transfer results depend on the thermal boundary-layer conditions applied in the solution. Therefore, consideration of convective heat transfer problems as conjugate problems is necessary to obtain physically more accurate results. An example of such conjugate problems is the thermal conjugation between two thermal fluid systems of free and forced convection separated by a vertical wall, which may be encountered in many engineering applications, such as nuclear reactor cooling, air conditioning systems, heat exchangers, and thermal buildings insulation. However, modeling a conjugate convection problem is complicated because it is necessary to solve simultaneously the energy and momentum equations of two convection modes with the wall heat conduction equation.

From the viewpoint of involved convection modes, conjugate free and forced convection problems may be classified into three categories: 1) two forced convection systems, 2) two free convection systems, and 3) a forced convection system and a natural convection system. Similar classification can be given for the conjugation between mixed convection and free or forced convection. The problems type of two forced convection systems was treated originally by Mori et al.,[1] who proved that the heat conduction in the separating wall affects the thermal interaction between the two systems. However, the analysis of this problem type is less complicated than the free convection part of categories 1 and 2. This is because the energy and momentum equations of forced convection layer can be solved separately, whereas those of free convection layer have to be solved simultaneously.

Many studies have been published on the subject of thermal conjugation between two natural convection systems.[2–10] Lock and Ko[2] did the first theoretical work by using the similarity transformation

technique with the finite difference method. They stated that the wall conduction has a remarkable effect on the thermal interaction process between the two convection systems. Later, Viskanta and Lankford[3] analyzed the same problem, based on the superposition principal, and derived results that were similar to those found by Lock and Ko. In another study, Sakakibara and Amaya[5] stated that the superposition technique is not adequate to treat such a conjugate problem because of the nonlinearity in the fundamental free convection equations. Perhaps a more important contribution in this research topic could be attributed to Anderson and Bejan[6] and Bejan and Anderson,[7,8] who used an Oseen analytic technique, modified originally by Gill,[10] to treat cases of this thermal conjugation type between 1) two Newtonian fluids, 2) two porous fluids, and 3) a porous fluid and a Newtonian fluid. In their approach, the separating wall was assumed either as a partition with negligible thermal resistance[6,7] or with finite thickness of considerable conduction resistance only in the transversal direction.

With respect to the thermal interaction between free and forced convection systems, a few studies have been published. The first work was reported by Sparrow and Faghri,[11] who numerically treated the coupled heat transfer between upward forced flow inside a vertical circular tube and the ambient natural convection, induced in the same direction, assuming the tube wall as a partition of negligible thermal resistance.

Mosaad[12] has analytically solved the problem of thermal interaction between two vertical systems of free and forced convection assuming the separating wall as a partition without thermal resistance. Thus, the problem was simplified into two adjacent free and convection layers, whose solutions were derived from using the same set of boundary conditions at the common fluid–fluid interface. In spite of this extreme simplification, the main advantage of such an analytical approach is that the parametric dependence of interactive heat transfer mechanisms is considerably more visible than in a numerical solution. However, to achieve better modeling for the physical reality of the investigated phenomenon, the wall heat conduction effect, neglected in our previous simple model,[12] has to be considered. Therefore, in the present work, free and forced convection layers are analyzed separately by applying the appropriate boundary conditions at the wall side facing the related convection layer. Then, the resultant two convection relations, which differed from those in the earlier model,[12] are coupled with the wall conduction solution to yield the conjugate problem solution.

II. Physical Model and Analysis

Consider two semi-infinite fluid media at different temperatures, which communicate thermally across a vertical separating wall of height L and thickness b. The cold fluid is at bulk temperature $t_{c\infty}$ and flows upward with free velocity u_∞ along one of two vertical wall sides. The hot fluid on the opposite side is stagnant and at free temperature $t_{h\infty} \gg t_{c\infty}$. As a result of heat transfer from the hot to the cold medium, a free convection boundary layer is induced on the hot side with flow counter to the forced-layer flow. This situation is shown in Fig. 1. For clarity, subscripts c, h, and w are used to specify variables and parameters belonging to the cold fluid, the hot fluid, and the wall, respectively.

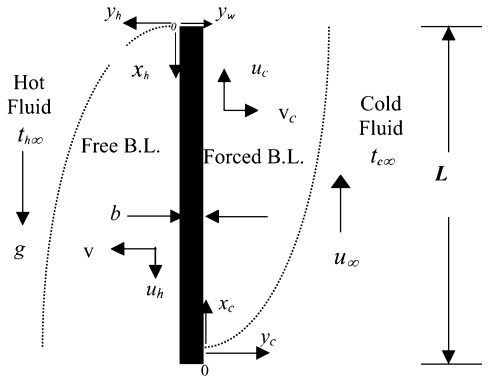

Fig. 1 Physical model.

In such cases, the development of two thermal boundary layers on wall sides depends on the interfacial temperature profile on both sides, which cannot be prescribed in the analysis; rather, it must be determined from the final conjugate solution. Thus, the stated problem seems to be complicated; therefore, the following simplifications of boundary-layer theory are introduced to simplify the analysis of two convection layers: 1) steady, laminar, two-dimensional flow in both layers; 2) negligible axial conduction and viscous dissipation; 3) zero external pressure gradients; 4) constant physical properties with application of the Boussinesq approximation for the free layer; and 5) hot fluid of $Pr_h \gg 1$ and cold fluid of $Pr_c = \mathcal{O}(1)$.

In addition, the wall heat conduction is assumed significant only in the transversal direction. A brief description of the analysis presented next: The forced convection layer is analyzed by the integral technique, whereas the free convection layer is analyzed by the Oseen technique. Then, the two analyses are coupled with the wall conduction solution by applying the interfacial conditions at the wall sides.

A. Forced Convection

The momentum and energy equations of the forced boundary layer can be expressed in dimensionless integral form,

$$\frac{\mathrm{d}}{\mathrm{d}X_c}\int_0^{\Delta} U_c(U_c-1)\,\mathrm{d}Y_c = -\left.\frac{\partial U_c}{\partial Y_c}\right|_{Y_c=0} \tag{1}$$

$$\frac{\mathrm{d}}{\mathrm{d}X_c}\int_0^{\Delta_t} U_c\left(\theta_c+\frac{1}{2}\right)\mathrm{d}Y_c = -\frac{1}{Pr_c}\left.\frac{\partial \theta_c}{\partial Y_c}\right|_{Y_c=0} \tag{2}$$

The dimensionless variables introduced are

$$X_c = x/L, \qquad Y_c = (y_c/L)Re_L^{\frac{1}{2}}, \qquad \Delta = (\delta/L)Re_L^{\frac{1}{2}}$$

$$\Delta_t = (\delta_t/L)Re_L^{\frac{1}{2}}, \qquad U_c = u_c/u_\infty$$

$$\theta_c = [t_c - 0.5(t_{h\infty}+t_{c\infty})]/\Delta t \tag{3}$$

where X_c and Y_c are dimensionless coordinates, whereas Δ and Δ_t are the dimensionless thickness of the velocity and the thermal boundary layer, respectively. U_c and θ_c are, respectively, the dimensionless fluid velocity and temperature. $\Delta t\ (=t_{h\infty}-t_{c\infty})$ is the total temperature drop across the two fluid media. $Re\ (=u_\omega L/\nu_c)$ is the Reynolds number and Pr_c is the Prandtl number of the cold fluid.

The velocity and temperature boundary conditions are, at $Y_c = 0$,

$$U_c = 0, \qquad \frac{\partial^2 U_c}{\partial Y_c^2} = 0, \qquad \theta_c = \theta_{wc}(X_c), \qquad \frac{\partial^2 \theta_c}{\partial Y_c^2} = 0 \tag{4a}$$

and at $Y_c = \Delta$,

$$U_c = 1, \qquad \frac{\partial U_c}{\partial Y_c} = 0, \qquad Y_c = \Delta_t, \qquad \theta_c = -\frac{1}{2}, \qquad \frac{\partial \theta_c}{\partial Y_c} = 0 \tag{4b}$$

where $\theta_{wc} = [(t_{wc} - 0.5(t_{h\infty}+t_{c\infty})]/\Delta t$ is the dimensionless local temperature of cold-wall side and is a function of the X_c coordinate.

The cubic velocity and temperature profiles satisfying boundary conditions (4) are, respectively,

$$U_c = \tfrac{3}{2}(Y_c/\Delta) - \tfrac{1}{2}(Y_c/\Delta)^3, \qquad 0 \le Y_c \le \Delta \tag{5}$$

$$\left(\theta_c+\tfrac{1}{2}\right)\Big/\left(\theta_{wc}+\tfrac{1}{2}\right) = 1 - \tfrac{3}{2}(Y_c/\Delta_t) + \tfrac{1}{2}(Y_c/\Delta_t)^3$$

$$0 \le Y_c \le \Delta_t \tag{6}$$

Solving Eqs. (1) and (2) for the velocity and temperature profiles yields, respectively,

$$\Delta = \sqrt{\frac{280X_c}{13}} \tag{7}$$

$$\frac{\mathrm{d}}{\mathrm{d}X_c}\left[\Delta_t\left(\theta_{wc}+\frac{1}{2}\right)\right]=\frac{10\left(\theta_{wc}+\frac{1}{2}\right)}{\left\{[\oslash-(\oslash^3/14)]Pr_c\Delta_t\right\}}\approx\frac{10\left(\theta_{wc}+\frac{1}{2}\right)}{\{\oslash Pr_c\Delta_t\}} \tag{8}$$

B. Free Convection

The equations governing mass, momentum, and energy in the free convection layer may be written, respectively, in dimensionless form as

$$\frac{\partial U_h}{\partial X_h}+\frac{\partial V_h}{\partial Y_h}=0 \tag{9}$$

$$\frac{\partial\theta_h}{\partial Y_h}=-\frac{\partial^3 U_h}{\partial Y_h^3} \tag{10}$$

$$U_h\frac{\partial\theta_h}{\partial X_h}+V_h\frac{\partial\theta_h}{\partial Y_h}=\frac{\partial^2\theta_h}{\partial Y_h^2} \tag{11}$$

The dimensionless variables and parameters introduced are

$$Y_h=y_h/l,\qquad X_h=1-X_c,\qquad U_h=u\Big/\left(\alpha_h L\Big/l^2\right)$$
$$V_h=v_h/(\alpha_h/l),\qquad Pr_h=\upsilon_h/\alpha_h$$
$$l=LRa^{-\frac{1}{4}},\qquad Ra=g\beta_h L^3\Delta t\Big/(\upsilon_h\alpha_h)$$
$$\theta_h=[t_h-0.5(t_{h\infty}+t_{c\infty})]/\Delta t \tag{12}$$

In the preceding equations, U_h and V_h are the velocity components in the X_h and Y_h directions, respectively, Ra is the modified Rayleigh number based on the total wall height L and the total temperature drop Δt. The variables β_h, υ_h, α_h, and Pr_h are, respectively, the thermal expansion coefficient, kinematic viscosity, thermal diffusivity, and Prandtl number of the hot fluid. The introduced scale of free-layer thickness, $l=Ra^{-1/4}$, satisfies the requirement of the boundary-layer theory that $l/L\ll 1$.

Equation (10) is derived by eliminating the pressure gradients between the x and y momentum equations after cross differentiating and subtracting those two equations.[6] The inertia terms in Eq. (10) are ignored relative to the body force and the viscous shear force. This scaling is valid[13] for $Pr_h\gg 1$.

The appropriate velocity and temperature boundary conditions at $Y_h=0$ are

$$U_h=V_h=0,\qquad \theta_h=\theta_{wh}(X_h) \tag{13}$$

For $Y_h\to\infty$,

$$U_h=0,\qquad \theta_h=\tfrac{1}{2} \tag{14}$$

where $\theta_{wh}=[(t_{wh}-0.5(t_{h\infty}+t_{c\infty})]/\Delta_t$ is the dimensionless local temperature of the wall side facing the hot fluid, which is a function of the X_h variable.

Following previous studies,[6,7,15,16] the modified Oseen technique of Gill[10] is employed for solving Eqs. (9–11) subject to boundary conditions (13) and (14). In this technique, the horizontal velocity component V_h and the temperature gradient $(\partial\theta_h/\partial X_h)$ in energy equation (11) are considered functions of the Y_h coordinate only. Accordingly, this energy equation can be coupled with the momentum equation (10) to yield an ordinary differential equation, whose analytical solution is

$$U_h=\left(\frac{1}{2}-\theta_{wh}\right)\frac{\left(e^{-\lambda Y_h}\sin\lambda Y_h\right)}{2\lambda^2} \tag{15}$$

$$\theta_h=\frac{1}{2}+\left(\theta_{wh}-\frac{1}{2}\right)e^{-\lambda Y_h}\cos\lambda\, Y_h \tag{16}$$

Velocity and temperature profiles (13) and (14) prove that the inverse of Oseen function $\lambda(X)$ plays the role of free-layer thickness.

From the condition that velocity and temperature solutions (15) and (16) with the V_h solution [obtained by integrating Eq. (9)] have to satisfy the integration of energy equation (11) across the layer, one gets the relation

$$\frac{\mathrm{d}}{\mathrm{d}X_h}\left[\frac{\left(\frac{1}{2}-\theta_{wh}\right)^2}{16\lambda^3}\right]=\lambda\left(\frac{1}{2}-\theta_{wh}\right) \tag{17}$$

For more detail on the Oseen procedure, see Ref. 7, among others. Here, note that the two final relations (8) and (17) involve four unknown parameters, θ_{wh}, λ, θ_{wc}, and Δ_t.

Wall Heat Conduction

For $L/b\gg 1$, the longitudinal heat conduction in the solid wall may be neglected compared with the transversal conduction.Hence, the wall heat conduction can be modeled by

$$\frac{\partial^2\theta_w}{\partial y_w^2}=0 \tag{18}$$

with boundary conditions, at $Y_w=0$,

$$\theta_w=\theta_{wh}(X_h) \tag{19}$$

and at $Y_w=1$,

$$\theta_w=\theta_{wc}(X_h) \tag{20}$$

The dimensionless variables are defined as

$$Y_w=y_w/b,\qquad \theta_w=[t_w-0.5(t_{h\infty}+t_{c\infty})]/(t_{h\infty}-t_{c\infty}) \tag{21}$$

Solution of Eq. (18) subject to Eqs. (19) and (20) is

$$\theta_w=\theta_{wh}-(\theta_{wh}-\theta_{wc})Y_w \tag{22}$$

Fluid–Solid Interface Conditions

At any vertical position x, the continuity of the heat flux and temperature at wall sides may be expressed as

$$k_h\frac{\partial t_h}{\partial y_h}\bigg|_{y_h=0}=-k_c\frac{\partial t_c}{\partial y_c}\bigg|_{y_c=0}=-k_w\frac{\partial t_w}{\partial y_w}\bigg|_{y_w=0} \tag{23}$$

The preceding equality can be rewritten in dimensionless form,

$$\zeta\frac{\partial\theta_h}{\partial Y_h}\bigg|_{Y_h=0}=-\frac{\partial\theta_c}{\partial Y_c}\bigg|_{Y_c=0}=\frac{\theta_{wh}-\theta_{wc}}{\omega} \tag{24}$$

The two dimensionless parameters introduced are defined as

$$\omega=(bk_c/Lk_w)Re_L^{\frac{1}{2}}\qquad \zeta=k_hRa_L^{\frac{1}{4}}\Big/k_cRe_L^{\frac{1}{2}} \tag{25}$$

The parameter ω relates the wall thermal resistance to the forced convection-layer resistance and ζ is the thermal resistance ratio of free and forced layers.

Inserting Eqs. (6) and (16) into Eq. (24) yields, after variables separation, the two relations

$$\theta_{wc}+\frac{1}{2}=\frac{2\zeta\Delta_t}{[3\eta+\zeta(3\omega+2\Delta_t)]} \tag{26}$$

$$\theta_{wh}-\frac{1}{2}=\frac{-3\eta}{[3\eta+\zeta(3\omega+2\Delta_t)]},\qquad \eta=\frac{1}{\lambda} \tag{27}$$

Inserting Eq. (26) into Eq. (8), and Eq. (27) into Eq. (17) for $X_h=1-X_c$, gives, aftersome mathematical manipulations, the

following two differential equations:

$$\frac{d\Delta_t^2}{dX_c} = \frac{10[9\eta + 5\zeta(2\Delta_t + 3\omega)]/(\phi Pr_c) - 16\Delta_t^2[3\eta + \zeta(2\Delta_t + 3\omega)]/\eta^4}{9\eta + 5\zeta(\Delta_t + 3\omega)} \tag{28}$$

$$\frac{d\eta^5}{dX_c} = \left\{ \frac{300\zeta\eta^5}{(\phi Pr_c\Delta_t)} - 80\left[9\eta^2 + 9\zeta(\Delta_t + 2\omega)\eta + \zeta^2(2\Delta_t + 3\omega)(\Delta_t + 2\omega)\right] \right\} \Big/ [27\eta + 15\zeta(\Delta_t + 3\omega)] \tag{29}$$

So far, Eqs. (26) and (29) are considered the more important results of the present analysis, whose solutions provide the distributions of the unknown parameters Δ_t, η, θ_{wh}, and θ_{wc} along the wall for certain values of ζ, ω, and Pr_c.

The local Nusselt number of the free convection side, $Nu_{xh} = (h_{xh}x_h/k_h)$, is defined by

$$\frac{Nu_{xh}}{Ra_x^{\frac{1}{4}}} = \frac{\sqrt{1 - Xc}}{(0.5 - \theta_{wh})} \left.\frac{\partial\theta_c}{\partial Y_h}\right|_{Y_h = 0} \tag{30}$$

Similarly, the local Nusselt number of the forced convection side, $Nu_{xc} = (h_{xc}x/k_c)$, is calculated by

$$\frac{Nu_{xc}}{\mathrm{Re}_x^{\frac{1}{2}}} = -\frac{\sqrt{X_c}}{(\theta_{wc} + 0.5)} \left.\frac{\partial\theta_c}{\partial Y_c}\right|_{Y_c = 0} \tag{31}$$

However, most important is the mean wall heat flux over the entire wall height, which is defined by

$$\bar{q} = \frac{k_h}{L}\int_1^0 \left.\frac{\partial t_h}{\partial y_h}\right|_{y_h = 0} dx_h = -\frac{k_c}{L}\int_0^1 \left.\frac{\partial t_c}{\partial y_c}\right|_{y_c = 0} dx_c \tag{32}$$

Relation (32) can be expressed in a dimensionless form related to the forced convection side, in terms of the mean conjugate Nusselt number $\overline{Nu} = \bar{q}L/(k_c\Delta t)$, as

$$\frac{\overline{Nu}}{Re_L^{\frac{1}{2}}Pr_c^{\frac{1}{3}}} = \frac{-1}{Pr_c^{\frac{1}{3}}}\int_0^1 \left.\frac{\partial\theta_c}{\partial Y_c}\right|_{Y_c = 0} dX_c \tag{33}$$

or related to the free convection side, in terms of $\overline{Nu} = \bar{q}L/(k_h\Delta t)$, as

$$\frac{\overline{Nu}}{Ra^{\frac{1}{4}}} = \int_0^1 \left.\frac{\partial\theta_h}{\partial Y_h}\right|_{Y_h = 0} dX_h \tag{34}$$

III. Solution and Results Discussion

Equations (28) and (29) are implicit and dependent differential equations involving two unknown parameters, Δ_t and η. Therefore, they have to be solved simultaneously to determine the distributions of Δ_t and η along the wall for certain values of ζ, ω and Pr_c. However, a simultaneous numerical integration of these two equations requires the boundary values of Δ_t and η at $X_c = 0$ to be known. Investigating Eqs. (15) and (16) reveals that the inverse Oseen function η $(=1/\lambda)$ plays the role of the dimensionless thickness of the free convection layer. Based on this and referring to Fig. 1, Δ_t has to assume zero value at $X_c = 0$ and a maximum value at $X_c = 1$, whereas η has to take a maximum value at $X_c = 0$ and zero value at $X_c = 1$. However, a numerical solution of Eq. (28) for $\Delta_t = 0$ at $X_c = 0$ may be impossible due to the singularity problem involved. Therefore, another appropriate initial value Δ_{t0} at $X_c = 0$ has to be used to overcome this problem of singularity. Solving Eq. (28) for $\Delta_t \to 0$ as $X_c \to 0$ yields

$$\Delta_{t0} = 0.9756\sqrt{280X_0/13}\Big/ Pr_c^{\frac{1}{3}}$$

where X_0 is a very small value of X_c. In addition, the maximum η value at $X_c = 0$ (Fig. 1) is unknown; therefore, this value should be estimated at the start of numerical integration.

The fourth-order Runge–Kutta integral procedure was employed to perform this numerical task. The integration starts at a small $X_c = X_0$ using an assumed value for $\eta_{\max}$ and $\Delta_t = \Delta_{t0}$, then advances in small steps ΔX_c until $X_c = 1$. When the predicted value of η at $X_c = 1$ is different from zero, the procedure is repeated using a new adjusted value for $\eta_{\max}$ until, eventually, the predicted η value at $X_c = 1$ becomes very close to zero. As a criterion to stop, the solution trials is that the predicted η value at $X_c = 1$ is less than 0.00001. It was found that the numerical solution with $X_0 = 0.0001$ and $\Delta X_c = 0.005$ gives stable and accurate results. Numerical results have been obtained for a matrix of discrete values of ζ, ω, and Pr_c.

First, the results obtained for the thin-wall case ($\omega \to 0$) are discussed. For this $\omega \to 0$ limit, Eqs. (26) and (27) yield, respectively, $\theta_{wc} \to -\frac{1}{2}$ and $\theta_{wh} \to -\frac{1}{2}$, as $\zeta \to 0$. Hence, Eq. (6) indicates that $\theta_c \to -\frac{1}{2}$. This means that, on the $\zeta \to 0$ limit, the temperature in the wall and forced convection layer becomes uniform and takes the low extreme value $-\frac{1}{2}$ of the cold fluid temperature. This implies that the two-fluid problem collapses to the classical one-fluid problem of free convection on an isothermal vertical surface. The relevant analytical solution of this extreme case can be derived by reworking the analysis of free convection part for $\theta_{wh} = -\frac{1}{2}$. This yields the mean Nusselt number formula,[13]

$$\overline{Nu}/Ra^{\frac{1}{4}} = 0.621 \tag{35}$$

This asymptotic result agrees within 2.5% with the similarity solution[14] for $Pr_h \to \gg 1$.

On the opposite extreme limit, $\zeta \to \infty$, Eqs. (26) and (27) for $\omega \to 0$ yield, respectively, $\theta_{wc} \to \frac{1}{2}$ and $\theta_{wh} \to \frac{1}{2}$. Hence, Eq. (16) shows that $\theta_h \to \frac{1}{2}$. Hence, the temperature in both the wall and free convection region takes the maximum extreme value one-half of the hot fluid. This means making the free convection layer disappear and reducing the problem to the classical one of forced convection on an isothermal vertical surface. The relevant solution can be deduced by reworking the part of the forced convection analysis for $\theta_{wc} = \frac{1}{2}$, which reads

$$\overline{Nu}\Big/\left(Re_L^{\frac{1}{2}}Pr_c^{\frac{1}{3}}\right) = 0.664 \tag{36}$$

Relation (36) is the same similarity solution[13] of forced convection on an isothermal surface recommended for $0.6 \le Pr_c \le 10$.

The two asymptotic results (35) and (36) obtained for the thin-wall limit prove the validity of present approach. In preliminary tests of the employed numerical technique, these two results were used as a reference to adjust the accuracy of solution as well as to ensure its reliability.

Numerical results obtained for the thin-wall case of $\omega = 0$ are shown in Fig. 2, where the distribution of temperature at both interface sides θ_{wh} and θ_{wc} are plotted for various values of ζ. In this

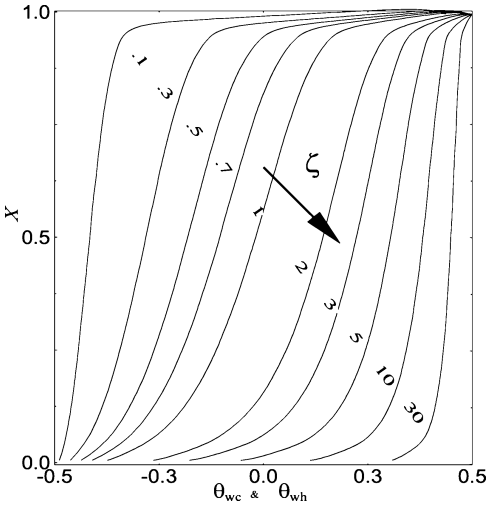

Fig. 2 Variation of interfacial temperature at interface sides with ζ parameter, for $\omega = 0$ and $Pr_c = 1$.

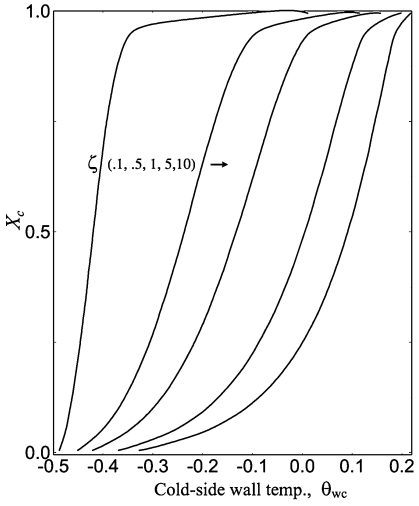

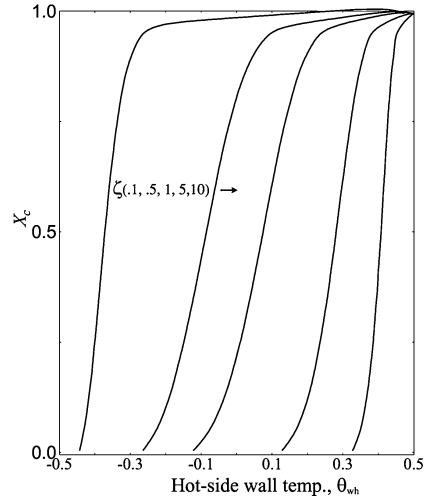

Fig. 3 Variation of interfacial temperature at wall sides with ζ parameter, $\omega = 1$ and $Pr_c = 1$.

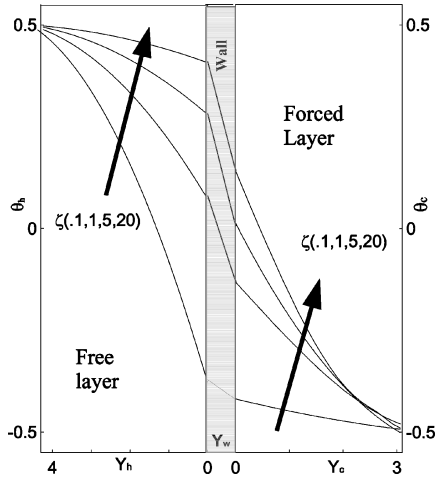

Fig. 4 Typical temperature profiles in wall and two fluid regions at midheight, $X = 0.5$, $\omega = 1$, and $Pr_c = 1$.

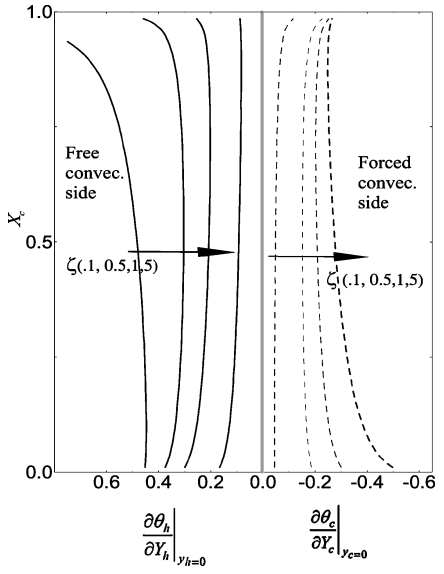

Fig. 5 Effect of ζ parameter on fluid temperature gradient at wall side, $Pr_c = 1$ and $\omega = 1$.

case, the separating wall is as a partition of zero thermal resistance. Therefore, the two predicted profiles of θ_{wh} and θ_{wc} are identical, and so they are represented by a common curve in Fig. 2. It was also found that for $\zeta \to 0$ or $\zeta \to \infty$ both θ_{wh} and θ_{wc} take nearly a uniform value over the entire wall height. This value is very close to $-\frac{1}{2}$ as $\zeta \to 0$ and very near to $\frac{1}{2}$ when $\zeta \to \infty$. However, for more clarity in presentation, the data plotted in Fig. 2 are restricted to $0.1 \le \zeta \le 30$.

Next, results obtained for the case of finite-thickness wall ($\omega > 0$) are discussed. The heat transfer characteristics of this real and more practical case are shown in Figs. 3–10. The variation of θ_{wh} and θ_{wc} along the wall sides with convective conjugation parameter ζ is shown in Fig. 3 for $\omega = 1$ and $Pr_c = 1$. It is clear that both θ_{wh} and θ_{wc} rise with the increase in ζ. This effect is more clearly shown in Fig. 4, where typical temperature profiles across the three regions are plotted at wall midheight for various ζ. These results show that the local interfacial temperature increases on both sides with the increase in ζ value. The results of Fig. 5 indicate that, for a higher value of ζ, the local fluid temperature gradient at wall surface assumes a higher value on forced convection side and a lower value on free convection side.

The effect of ω parameter on the interfacial temperature at the wall sides is shown in Fig. 6. It is clear that, at a fixed vertical position, increasing ω decreases θ_{wc}, whereas increases θ_{wh}, that is, the temperature drop across the wall increases with ω due to the increase in its resistance. The wall acts as a thermal insulator between the two fluid media. The data plotted in Fig. 7 show that, for a higher ω value, the local fluid temperature gradient at both wall sides assumes a lower value over the entire height. Note that, for a fixed ω value, this gradient assumes a maximum value at the start point of the boundary layer, which decreases with altitude due to the development of layer thickness (compare Fig. 8).

The effect of the Prandtl number Pr_c of cold fluid on the thickness of free and forced convection layer is presented in Fig. 8. It is clear that for a higher Pr_c forced-layer thickness becomes thinner, whereas no significant effect is noted on free-layer thickness.

Numerical data obtained for the local Nusselt number of the forced convection side Nu_x [Eq. (31)] are shown in Fig. 9 for various values of ω. These data are bounded by the two known exact results of forced convection on surfaces with uniform temperature and uniform heat flux. It is clear that the numerical solution approaches the exact uniform heat flux solution as ω increases. A similar conclusion can be made on the effect of the ω parameter on the local Nusselt number of free convection Nu_{xh} [Eq. (30)]. However, the graph is not presented in the interest of saving space.

Numerically obtained values for the mean conjugate Nusselt number $\overline{Nu}$, defined by Eq. (33), are shown in Fig. 10 as a function of ω and ζ parameters. In Fig. 10, the first upper curve of $\omega = 0$ is bounded by the two asymptotic lines of solutions (35) and (36) of free and forced convection on isothermal surfaces. This $\omega = 0$ result is the same as of the model[12] of negligible wall thermal resistance. This proves the validity of present approach. The numerical data

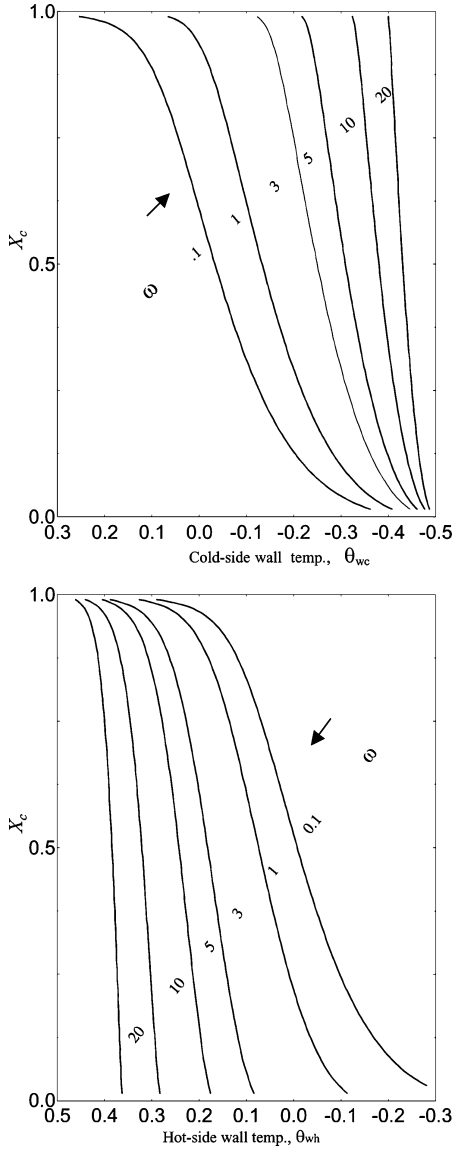

Fig. 6 Effect of ω parameter on interface temperatures at wall sides, $Pr_c = 1$ and $\zeta = 1$.

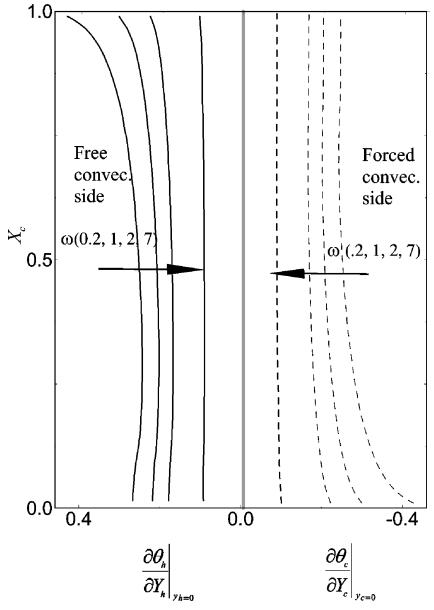

Fig. 7 Effect of ω parameter on fluid temperature gradient at wall sides, $Pr_c = 1$ and $\zeta = 1$.

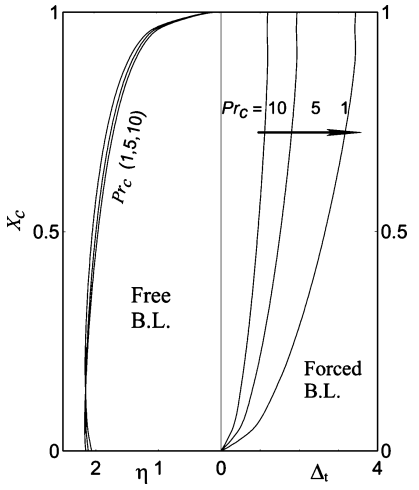

Fig. 8 Effect of cold-fluid Prandtl number on thickness of convection layer on both fluid sides, $\omega = 0.5$ and $\zeta = 1$.

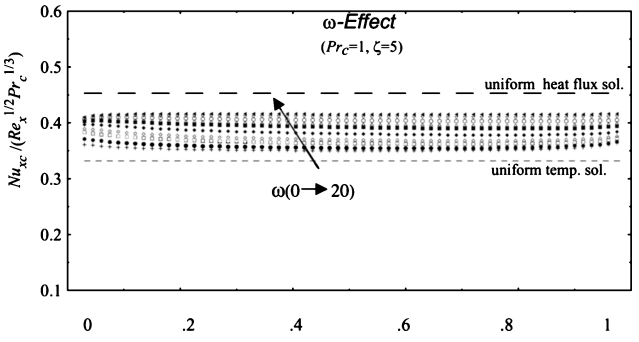

Fig. 9 Dependence of local Nusselt number of forced convection side on ω.

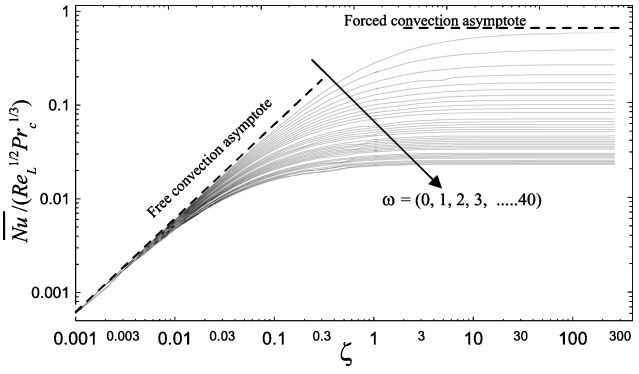

Fig. 10 Mean conjugate Nusselt number as function of ζ and ω.

plotted Fig. 10 show that the mean conjugate Nusselt number $\overline{Nu}$ increases with ζ, whereas it decreases with ω.

For $0 \le \omega \le 5$ and $0 \le \zeta < 100$, these data could be correlated using a fit process within $\pm 9.8\%$ by

$$\overline{Nu}/(Re^{\frac{1}{2}}Pr^{\frac{1}{3}}) = \left[0.621\zeta e^{-\zeta^{0.531}} + 0.664\left(1 - e^{-0.093\zeta^{0.926}}\right)\right]F(\omega)$$

$$F(\omega) = 1 - 0.00132(1 + 0.27\omega^{0.15}\zeta^{0.1})^{20.749}, \qquad 0 \le \zeta \le 1$$

$$F(\omega) = 1 - 0.00037\left(1 + \frac{0.5\omega^{0.15}\zeta^{0.025}}{(1 + \omega^{0.15}\zeta^{0.025})}\right)^{29.927}, \qquad 1 < \zeta < 100 \tag{37}$$

For the thin-wall limit, this correlation reduces to relations (35) and (36) of free and forced convection on isothermal surfaces, for $\zeta \to 0$ and $\zeta \to \infty$, respectively.

IV. Model Validity

To this point, it has been proven that for the thin-wall limit of $\omega = 0$ the present model validates the previous model[12] of negligible wall resistance as well as yields, as special solutions, the well-known relations (35) and (36) of free and forced convection on isothermal surfaces. However, to the author's knowledge, there is no other relevant work available in literature that can be used to make comparisons to conduct further tests on present model validity. Therefore, a special model problem was constructed and solved numerically by the well-known numerical FLUENT program. With reference to Fig. 1, the data used in constructing this problem are a standard oil engine at $T_{h\infty} = 80°\text{C}$ as the hot fluid, water at $T_{c\infty} = 40°\text{C}$ with $u_\infty = 0.3$ m/s as the cold fluid, and a steel sheet [$L = 0.3$, $b = 1.5$ mm or 4 mm, $k = 14$ W/(m$^2 \cdot$ K)] as the separating wall. For the two cases of 1.5- and 4-mm wall thickness, comparisons between FLUENT and model results are presented in Figs. 11 and 12, respectively. For the case of thin-steel sheet ($b = 1.5$ mm, $\omega = 0.11$, and $\zeta = 0.22$), the comparison shown in Fig. 11 indicates good agreement between the two solutions, with deviation less than 2%. However, for the thick sheet ($b = 4$ mm, $\omega = 0.29$, and $\zeta = 0.22$), the comparison presented in Fig. 12 shows a considerable difference between the two solutions. This discrepancy between the two solutions is of average relative value of about 9%, which may be attributed to the effect of longitudinal wall conduction that was neglected in the analytical model.

As a brief conclusion, for the numerical FLUENT solution, the basic equations governing mass, momentum, and energy in the two cocurrent convection layers were solved numerically, under the same boundary-layer simplifications adopted in the analytical model, by using a control volume discretization procedure. A second-order upwind formula was used as the discretization scheme for the energy and momentum equations. The body force weighted scheme was used as the pressure interpolation scheme. A SIMPLEC algorithm[17,18] was used as the method for pressure–velocity coupling. A segregated solver was employed for simultaneous solution of the numerical form of the governing equations; underrelaxation factors were employed for all equations to control the solution convergence. The adopted convergence criteria were a variation of less than 10^{-7} in temperature and less than 10^{-6} in velocity over all grid points. A quadrilateral cell with successive ratio of 1.02 was determined for all edges throughout the domain, except equally spaced nodes were used in the solid slab that separates the two fluid regions. The numerical model was validated with the known exact solutions of laminar free and forced convection on vertical walls with known uniform surface temperature.

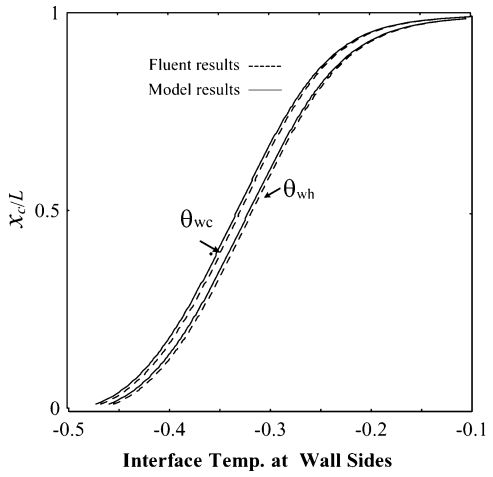

Fig. 11 Comparison of model predictions with FLUENT results for special model problem of thin wall, $b = 1.5$ mm, $\omega = 0.11$, and $\zeta = 0.22$.

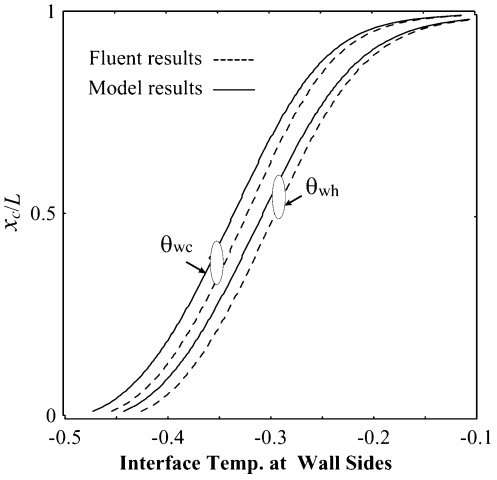

Fig. 12 Comparison of model predictions with FLUENT results for special model problem of thick wall, $b = 4$ mm, $\omega = 0.29$, and $\zeta = 0.22$.

V. Conclusions

The thermal communication between two vertical systems of free and forced convection has been analyzed by considering the heat conduction across the separating wall. The main points deduced from this work are as follows.

1) For the thin-wall limit, the present model validates the previous modelof negligible wall resistance and yields, as special solutions, the known expressions of calculating mean Nusselt numbers of free convection and forced convection on isothermal vertical surfaces.

2) Wall resistance relaxes the thermal interaction process between the two convection systems. The temperature drop across the separating wall is higher for a higher value of wall parameter ω.

3) An implicit expression has been found by means of a data-fit procedure for calculating the mean conjugate Nusselt number over the entire wall height as a function of ω and ζ parameters. This mean number increases with ζ and decreases with ω.

4) Comparison between numerical results, calculated by FLUENT for special model problems and present model predictions, has indicated a reasonable agreement, especially for small ω values.

References

[1]Mori, S., Kataya, M., and Tanimoto, A., "Performance of Counter flow, Parallel Plate Heat Exchangers Under Laminar Flow Conditions," *Heat Mass Transfer Engineering*, Vol. 2, No. 1, 1980, pp. 28–38.

[2]Lock, G., and Ko, R. S., "Coupling Through a Wall Between Two Free Convection Systems," *International Journal of Heat and Mass Transfer*, Vol. 16, May 1973, pp. 2087–2096.

[3]Viskanta, R., and Lankford, D. W., "Coupling of Heat Transfer Between Two Natural Convection Systems Separated by a Vertical Wall," *International Journal of Heat and Mass Transfer*, Vol. 24, June 1981, pp. 1171–1177.

[4]Trevino, C., Mendez, F., and Higuera, F. G., "Heat Transfer Across a Vertical Wall Separating Two Fluids at Different Temperatures," *Journal of Heat and Mass Transfer*, Vol. 39, No. 11, 1996, pp. 2231–2241.

[5]Sakakibara, M., and Amaya, H., "Conjugate Heat Transfer Between Two Vertical Natural Convection Reservoirs Separated by a Vertical Wall," *International Journal of Heat and Mass Transfer*, Vol. 35, No. 9, 1992, pp. 2289–2297.

[6]Anderson, R., and Bejan, A., "Natural Convection on Both Sides of a Vertical Wall Separating Fluids at Different Temperatures," *Journal of Heat Transfer*, Vol. 102, Nov. 1980, pp. 630–635.

[7]Bejan, A., and Anderson, R., "Heat Transfer Across a Vertical Impermeable Partition Imbedded in Porous Medium," *International Journal of Heat and Mass Transfer*, Vol. 24, No. 7, 1981, pp. 1237–1245.

[8]Bejan, A., and Anderson, R., "Natural Convection at the Interface Between a Vertical Porous Layer and an Open Space," *Journal of Heat Transfer*, Vol. 105, Feb. 1983, pp. 124–120.

[9]Bejan, A., "Note on Gill's Solution for Free Convection in a Vertical Enclosure," *Journal of Fluid Mechanics*, Vol. 90, May 1979, pp. 561–568.

[10]Gill, A. E., "The Boundary Layer Regime for Convection in a Rectangular Cavity," *Journal of Fluid Mechanics*, Vol. 26, March 1966, pp. 515–536.

[11]Sparrow, E. M., and Faghri, M., "Fluid-to-Fluid Conjugate Heat Transfer for a Vertical Pipe-Internal Forced Convection and External Natural Convection," *Journal of Heat Transfer*, Vol. 102, Aug. 1980, pp. 402–407.

[12]Mosaad, M., "Thermal Interaction Between Natural Convection on One Side of a Vertical Wall and Forced Convection on the Other Side," *Heat and Mass Transfer*, Vol. 35, May 1999, pp. 451–457.

[13]Baehr, F. D., and Stephan, K., *Heat and Mass Transfer*, Springer, Berlin, 1998, Chap. 3.

[14]Sparrow, E. M., and Gregg, J. L., "Laminar Free Convection for a Vertical Surface with Uniform Surface Heat Flux. Trans.," *Journal of Heat Transfer*, Vol. 78, Aug. 1965, pp. 435–440.

[15]Poulikakos, D., "Interaction Between Film Condensation on One Side of a Vertical Wall and Natural Convection on the Other Side," *Journal of Heat Transfer*, Vol. 108, Aug. 1986, pp. 560–566.

[16]Mosaad, M., "Natural Convection in a Porous Medium Coupled Across an Impermeable Vertical Wall with Film Condensation," *Heat and Mass Transfer*, Vol. 35, Jan. 1999, pp. 177–183.

[17]Vandoormaal, J. P., and Raithby, G. D., "Enhancements of the SIMPLE Method for Predicting Incompressible Fluid Flows," *Numerical Heat Transfer*, Vol. 7, 1964, pp. 147–163.

[18]Chen, X., and Han, P., "A Note on the Solution of Conjugate Heat Transfer Problems Using Simple-like Algorithms," *International Journal of Heat and Fluid Flow*, Vol. 21, 2002, pp. 463–467.